SENTINEL-2A red-edge spectral indices suitability for discriminating burn severity

Article *in* International Journal of Applied Earth Observation and Geoinformation · August 2016

DOI: 10.1016/j.jag.2016.03.005

3 authors:

Alfonso Fernandez-manso
Universidad de León
162 PUBLICATIONS **1,180** CITATIONS
SEE PROFILE

Oscar Fernández-Manso
Junta de Castilla y León
39 PUBLICATIONS **347** CITATIONS
SEE PROFILE

C. Quintano
Universidad de Valladolid
99 PUBLICATIONS **1,007** CITATIONS
SEE PROFILE

International Journal of Applied Earth Observation and Geoinformation 50 (2016) 170–175

Contents lists available at ScienceDirect

International Journal of Applied Earth Observation and Geoinformation

journal homepage: www.elsevier.com/locate/jag

SENTINEL-2A red-edge spectral indices suitability for discriminating burn severity

Alfonso Fernández-Manso[a], Oscar Fernández-Manso[b], Carmen Quintano[c,d,*]

[a] Agrarian Science and Engineering Department, University of León, Spain
[b] Civil Protection Agency, Castilla y León Government, Valladolid, Spain
[c] Electronic Technology Department, University of Valladolid, Spain
[d] Sustainable Forest Management Research Institute, University of Valladolid-Spanish National Institute for Agricultural and Food Research and Technology, Spain

ARTICLE INFO

Article history:
Received 8 February 2016
Received in revised form 16 March 2016
Accepted 18 March 2016

Keywords:
Sentinel-2
Burn severity
Red-edge
Spectral indices
Mediterranean

ABSTRACT

Fires are a problematic and recurrent issue in Mediterranean ecosystems. Accurate discrimination between burn severity levels is essential for the rehabilitation planning of burned areas. Sentinel-2A MultiSpectral Instrument (MSI) record data in three red-edge wavelengths, spectral domain especially useful on agriculture and vegetation applications. Our objective is to find out whether Sentinel-2A MSI red-edge wavelengths are suitable for burn severity discrimination. As study area, we used the 2015 Sierra Gata wildfire (Spain) that burned approximately 80 km^2. A Copernicus Emergency Management Service (EMS)-grading map with four burn severity levels was considered as reference truth. Cox and Snell, Nagelkerke and McFadde pseudo-R^2 statistics obtained by Multinomial Logistic Regression showed the superiority of red-edge spectral indices (particularly, Modified Simple Ratio Red-edge, Chlorophyll Index Red-edge, Normalized Difference Vegetation Index Red-edge) over conventional spectral indices. Fisher's Least Significant Difference test confirmed that Sentinel-2A MSI red-edge spectral indices are adequate to discriminate four burn severity levels.

1. Introduction

Remote sensing techniques have proven their usefulness to accurately estimate fire-affected areas and burn severity (Chuvieco, 2009). In this context, the Europe's Copernicus environmental monitoring programme Sentinel-2 gives continuity to the multispectral high-resolution optical observations over global terrestrial surfaces provided by the European Space Agency (ESA) through the SPOT series of satellites (Fletcher, 2012). Sentinel-2A, the first of the two-satellite Sentinel-2 mission, was launched on 23 June, 2015; Sentinel-2B will be launched in 2016. Some scientific journals had special issues dedicated to Sentinel-2 (e.g. Berger and Aschbacher, 2012), and many papers have proven the utility of Sentinel-2A data on different research lines (e.g. van der Werff and van der Meer, 2015; van der Meer et al., 2014).

Fires consume vegetation, destroy chlorophyll, alter soil moisture and leave bare soil. The chlorophyll decrease lead to changes in the visible, the red-edge and the near-infrared (NIR) wavelengths (Escuin et al., 2008). Most studies involving burn severity and remotely sensed data are based on red, NIR and shortwave infrared (SWIR) spectral regions (Chuvieco, 2009). Few works have, however, related the red-edge spectral domain with burn severity, mainly due to the low availability of red-edge remote sensed data of an acceptable spatial resolution. Chuvieco et al. (2006) stated that standard indices based on red and NIR bands (as Normalized Difference Vegetation Index, NDVI) increase its correlation to burn severity when using the upper part of the red band (red-edge). Korets et al. (2010) showed that red-edge based indices (indicators of chlorophyll content) are useful for quantifying and mapping forest damage due to fires in Siberia.

The MultiSpectral Instrument (MSI) onboard Sentinel-2A records data in the vegetation red-edge spectral domain, that is one of the best remote sensing based descriptors of chlorophyll content (Curran et al., 1990), providing an opportunity to assess red-edge spectral indices for burn severity discrimination. Thus, our work aims to find out whether Sentinel-2A MSI data is suitable to quantify burn severity in Mediterranean forest ecosystems. Particularly, our goal is to evaluate the potential of their red-edge spectral bands and to determine which Sentinel-based red-edge spectral indices

* Corresponding author at: Electronic Technology Department, University of Valladolid, Spain.
E-mail address: menchu@tele.uva.es (C. Quintano).

http://dx.doi.org/10.1016/j.jag.2016.03.005
0303-2434/

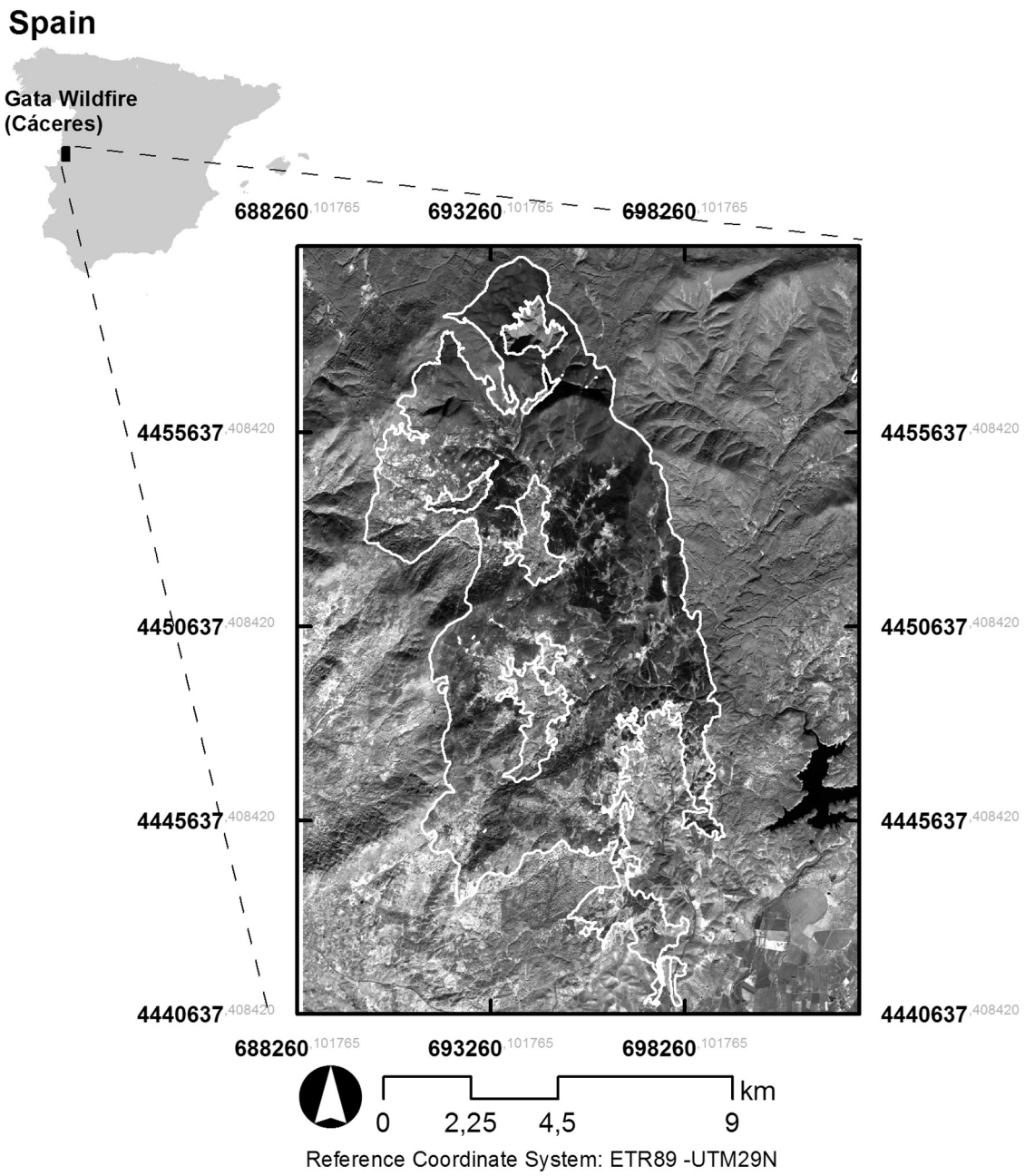

Fig. 1. Location of study area. Copernicus EMS-based burned area perimeter (white line) overlapping a Sentinel-2A MSI red-edge 1 spectral band (B5) image.

are more adequate to discriminate burn severity levels. This study is the first work that relates Sentinel-2A MSI images with burn severity.

2. Materials

The study area is located in Sierra de Gata (central-western Spain) where a wildfire happened from 6 to 11 August, 2015 burning 79.50 km^2 according to the Copernicus European program (Fig. 1). Affected vegetation was mainly a combination of shrubland and forest dominated by *Pinus pinaster* Ait. and *Quercus pyrenaica* Wild.

A Sentinel-2A MSI image (processing level 1C) acquired on 29 November, 2015 was downloaded from the ESA Sentinels Scientific Data Hub. The processing level 1C includes radiometric and geometric corrections with sub-pixel accuracy (ESA, 2015).

A Copernicus EMS-grading map (ID: EMSR132) was considered as reference truth. The map displays four levels of burn severity: destroyed area (level 3); highly damaged area (level 2), moderately damaged area (level 1); and negligible to slight damaged area (level 0). It was based on Pléiades-1A/1B data (acquired on 15 August, 2015) visual interpretation and validated by field plots with an estimated overall accuracy over 85%.

3. Method

The Sentinel-2A MSI bands were scaled to surface reflectance by a Dark Object Subtraction (DOS) based atmospheric correction (Chavez, 1996). Its spatial resolution was homogenized to 10 m using nearest neighbour resampling. Next, red-edge spectral indices were computed. We based our selection on the works about simulated Sentinel-2 data of Hill (2013) and Segl et al. (2015) and

Table 1
Cox and Snell, Nagelkerke and McFadden pseudo-R^2 statistics for Sentinel-2A MSI original bands and spectral indices (mainly based on red-edge wavelengths).

Acronym	Band	Central wavelength (nm)	Cox and Snell pseudo-R^2	Nagelkerke pseudo-R^2	McFadden pseudo-R^2
Original spectral bands					
B2	Blue	490	0.111	0.119	0.043
B3	Green	560	0.252	0.269	0.105
B4	Red	665	0.093	0.099	0.035
B5	Red-edge 1	705	0.311	0.332	0.134
B6	Red-edge 2	740	0.586	0.625	0.319
B7	Red-edge 3	783	0.606	0.646	0.337
B8	NIR	842	0.633	0.676	0.363
B8a	NIR narrow	865	0.625	0.667	0.355
B11	SWIR1	1610	0.134	0.143	0.052
B12	SWIR2	2190	0.175	0.180	0.028
Acronym	Spectral Index	Equation	Cox and Snell pseudo-R^2	Nagelkerke pseudo-R^2	McFadden pseudo-R^2
Reference spectral indices					
NDVI	Normalized Difference Vegetation Index	$\frac{(B8-B4)}{(B8+B4)}$	0.430	0.447	0.289
NBR	Normalized Burn Ratio	$\frac{(B8-B12)}{(B8+B12)}$	0.450	0.469	0.247
GNDVI	Green Normalized Difference Vegetation Index	$\frac{(B8-B3)}{(B8+B3)}$	0.532	0.576	0.296
SR	Simple Ratio	$\frac{B8}{B4}$	0.427	0.462	0.217
DVI	Difference Vegetation Index	$(B8 - B4)$	0.579	0.628	0.338
Red-edge spectral indices					
NDVIre1	Normalized Difference Vegetation Index red-edge 1	$\frac{(B8-B5)}{(B8+B5)}$	0.601	0.535	0.252
NDVIre1n	Normalized Difference Vegetation Index red-edge 1 narrow	$\frac{(B8a-B5)}{(B8a+B5)}$	0.600	0.533	0.251
NDVIre2	Normalized Difference Vegetation Index red-edge 2	$\frac{(B8-B6)}{(B8+B6)}$	0.158	0.168	0.062
NDVIre2n	Normalized Difference Vegetation Index red-edge 2 narrow	$\frac{(B8a-B6)}{(B8a+B6)}$	0.174	0.186	0.069
NDVIre3	Normalized Difference Vegetation Index red-edge 3	$\frac{(B8-B7)}{(B8+B7)}$	0.035	0.038	0.013
NDVIre3n	Normalized Difference Vegetation Index red-edge 3 narrow	$\frac{(B8a-B7)}{(B8a+B7)}$	0.012	0.012	0.004
PSRI	Plant Senescence Reflectance Index	$\frac{(B4-B3)}{B6}$	0.377	0.403	0.171
CIre	Chlorophyll Index red-edge	$\frac{B7}{B5} - 1$	0.683	0.653	0.512
NDre1	Normalized Difference red-edge 1	$\frac{(B6-B5)}{(B6+B5)}$	0.434	0.463	0.206
NDre1m	Normalized Difference red-edge 1 modified	$\frac{(B6-B5)}{(B6+B5-2B1)}$	0.234	0.250	0.097
NDre2	Normalized Difference red-edge 2	$\frac{(B7-B5)}{(B7+B5)}$	0.463	0.495	0.225
NDre2m	Normalized Difference red-edge 2 modified	$\frac{(B7-B5)}{(B7+B5-2B1)}$	0.432	0.448	0.196
SRre1	Simple Ratio red-edge 1	$\frac{(B6-B1)}{(B5-B1)}$	0.173	0.184	0.069
SRre2	Simple Ratio red-edge 2	$\frac{(B7-B1)}{(B5-B1)}$	0.169	0.180	0.067
MSRre	Modified Simple Ratio red-edge	$\frac{(B8/B5)-1}{\sqrt{(B8/B5)+1}}$	0.591	0.584	0.245
MSRren	Modified Simple Ratio red-edge narrow	$\frac{(B8a/B5)-1}{\sqrt{(B8a/B5)+1}}$	0.690	0.623	0.244

on the work of Shang et al. (2015) regarding RapidEye red-edge band. Specifically, we considered: Normalized Difference Vegetation Index Red-edge 1 (NDVIre1) (Gitelson and Merzlyak, 1994); Normalized Difference Vegetation Index Red-edge 2, (NDVIre2), similar to NDVIre1 but using red-edge band B6 instead of B5, proposed in this paper; their version using the narrow NIR band (B8a) (NDVIre1n, and NDVIre2n, respectively), proposed by us as well; Plant Senescence Reflectance Index (PSRI) (Merzlyak et al., 1999); Chlorophyll Index Red-edge (CIre) (Gitelson et al., 2003); Normalized Difference Red-edge 1 (NDre1) (Gitelson and Merzlyak, 1994); Normalized Difference Red-edge 2 (NDre2) (Barnes et al., 2000); their modified versions (NDre1m and NDre2m) (Sims and Gamon, 2002); Simple Ratio red-edge 1 and 2 (SRre1 and SRre2) (Sims and Gamon, 2000); Modified Simple Ratio red-edge (MSRre) (Chen, 1996); and its narrowed version (MSRren), proposed by us. In addition, we included Normalized Difference Vegetation Index (NDVI) (Tucker, 1979), Normalized Burn Ratio (NBR) (Key and Benson, 2006), Green NDVI (GNDVI) (Buschmann and Nagel, 1993), Simple Ratio (SR) (Birth and McVey, 1968), and Difference Vegetation Index (DVI) (Tucker, 1979) as a reference indices. As NDVI and NBR are known for their saturation effect at denser vegetation covers, GNDVI, SR and DVI, more sensitive for denser canopies, were used as well.

A total of 400 plots, 100 per burn severity level, were defined on the reference ground image by stratified random sampling. To minimize the possible registration errors between the Sentinel-2A MSI data and the Copernicus EMS-grading map used as reference ground, we applied a mean 3×3 filter to the original bands/spectral indices as a prior step to the extraction of digital values. One-way analysis of variance (ANOVA) and Fisher's Least Significant Difference (LSD) tested whether Sentinel-2A MSI data enable us to significantly distinguish the four burn severity levels. Additionally, the relationship between red-edge bands/spectral indices and burn severity was measured by Cox and Snell, Nagelkerke and McFadde pseudo-R^2 statistics obtained by Multinomial Logistic Regression (MLR) when categorical burn severity level acted as response variable and red-edge bands/spectral indices as explanatory variables. Pseudo-R^2 statistics do not calculate the goodness of fit of the model

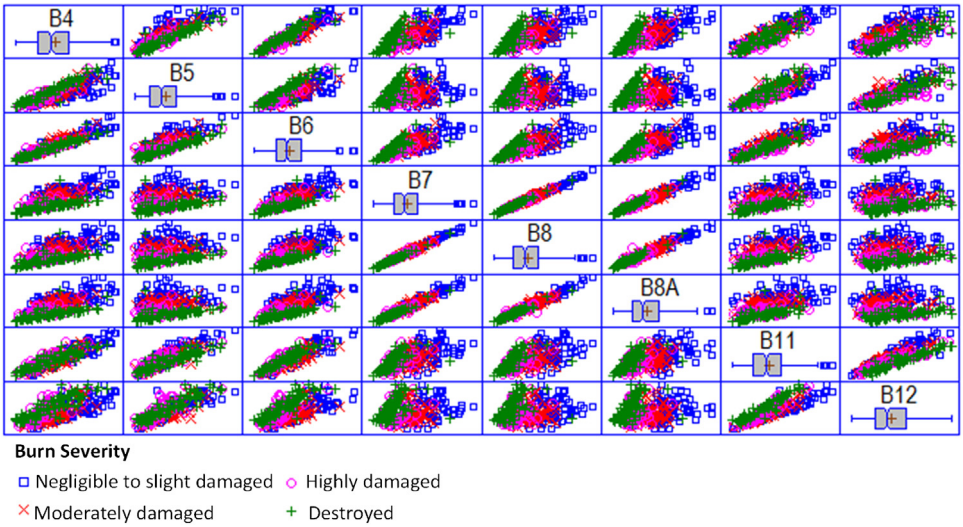

Fig. 2. Matrix of Sentinel-2A MSI spectral band scatterplots for the reference plots (four burn severity levels).

but rate the usefulness of the explanatory variables to predict the response variable (Agresti, 2002).

4. Results

We used a matrix plot to represent the Sentinel-2A MSI spectral bands scatterplots considering the four burn severity levels of the reference plots (Fig. 2). The matrix plot enabled us to gain an initial look at Sentinel-2A MSI spectral bands versus burn severity. Scatterplots among B7, B8 and B8a are almost linear displaying the high correlation between the bands. Conversely, scatterplots between B5 and B7, B8 or B8a have a triangular shape, and show very few confusion among the different burn severity levels. Scatterplots between B11 or B12 and B7, B8 or B8a have also a triangular shape but exhibit a higher confusion among burn severity levels.

Cox and Snell, Nagelkerke and McFadde pseudo-R^2 statistics from MLR are shown in Table 1. NIR bands together to red-edge bands B7 and B6 displayed the highest values. Surprisingly, pseudo-R^2 statistics of SWIR bands showed very low values. Regarding spectral indices, the NDVI versions based on red-edge wavelengths close to red, B5, (NDVIre1, NDVIre1n) provided higher pseudo-R^2 statistics than NDVI. Similar pseudo-R^2 values (though slightly higher) were found when other spectral indices also based on NIR bands and B5 were considered (MSRre, MSRren). CIre (based on two red-edge bands, one close to red and another close to NIR) displayed also high pseudo-R^2 statistics values (the highest Nagelkerke and McFadde, and the second highest Cox and Snell). NDre2 and NDre2m (based on the same spectral bands than CIre), however, showed intermediate pseudo-R^2 values, similar to NDVI, NBR or SR, and slightly lower than GNDI or DVI.

We did not find important differences between NDVI based on broadband NIR band B8 and the same indices based on the narrowband NIR band B8a. When considering NDVIre1, and NDVIre2, the narrow version had similar pseudo-R^2 statistics values to the broadband version. However, when considering MSRre the narrow version provided higher pseudo-R^2 statistics values.

Fisher's LSD test results are shown graphically by error-bar plots in Fig. 3. The performance of each spectral index totally agreed with the MLR results. NDVI and NBR allowed significant discrimination of the four burn severity levels, though levels 0 and 1 are difficult to distinguish due to the known NDVI and NBR saturation effect at denser vegetation. Reduction of the saturation effect can be observed when replacing the red band by the green band, GNDVI, and when considering DVI and SR, both known to be more sensitive for denser canopies. Replacing the red band by a red-edge band will decrease the saturation effect as well, as is shown in Fig. 3 (NDVIre1, NDVIre1n). PSRI showed confusion between level 0 and 1, and NDre1m, NDre2m, SRre1 and SRre2 between level 1 and 2. Conversely, CIre, NDre1, NDre2, MSEre and MSERren discriminated significantly the four burn severity levels.

5. Discussion and conclusion

GNDVI and DVI exhibited higher pseudo-R^2 statistics values than NDVI or NBR, indices commonly used to map burn severity, probably due to their higher sensitivity for denser canopies. However, red-edge spectral indices based on B5 and B7/B8 showed the highest suitability for burn severity discrimination. Specifically, CIre, a spectral index designed to estimate the chlorophyll content, displayed the maximum adequacy. Our results agree with the findings of Chuvieco et al. (2006), who observed that NDVI displayed a weaker correlation with burn severity than the NDVI version based on red-edge wavelengths close to red (NDVIre1, NDVIre1) and of Korets et al. (2010) that distinguished five post-fire tree mortality levels from a chlorophyll index. Contrary to Chuvieco et al. (2006), we obtained low pseudo-R^2 statistics values in SWIR bands. It may be due to two facts: the burned area comprised a big extension of shrubs and agricultural lands and not only forest, and the time elapsed since the fire resulted in a charcoal removal.

Our study validated Sentinel-2A MSI images to quantify burn severity. Particularly, it demonstrated the adequacy of their red-edge wavelengths. Both Fisher's LSD test and pseudo-R^2 statistics from MLR showed that Sentinel-2A MSI red-edge spectral indices discriminated significantly four burn severity levels in Mediterranean forest ecosystems. We conclude that the most suitable Sentinel-2A MSI spectral indices to discriminate burn severity are the indices based on B5, red-edge close to red wavelengths mainly associated to variations in chlorophyll content, and B7 or B8, red-edge close to NIR or NIR, mainly related to variations in leaf structure. Sentinel-2A MSI data, with higher spectral, spatial and temporal resolutions than Landsat-8 OLI data (a reference for burn severity studies), may contribute to evaluate accurately burn severity, and to increase the adequacy of fire management strategies. However, future research is needed to extend the conclusions of this preliminary work to other fire regimes and ecosystems.

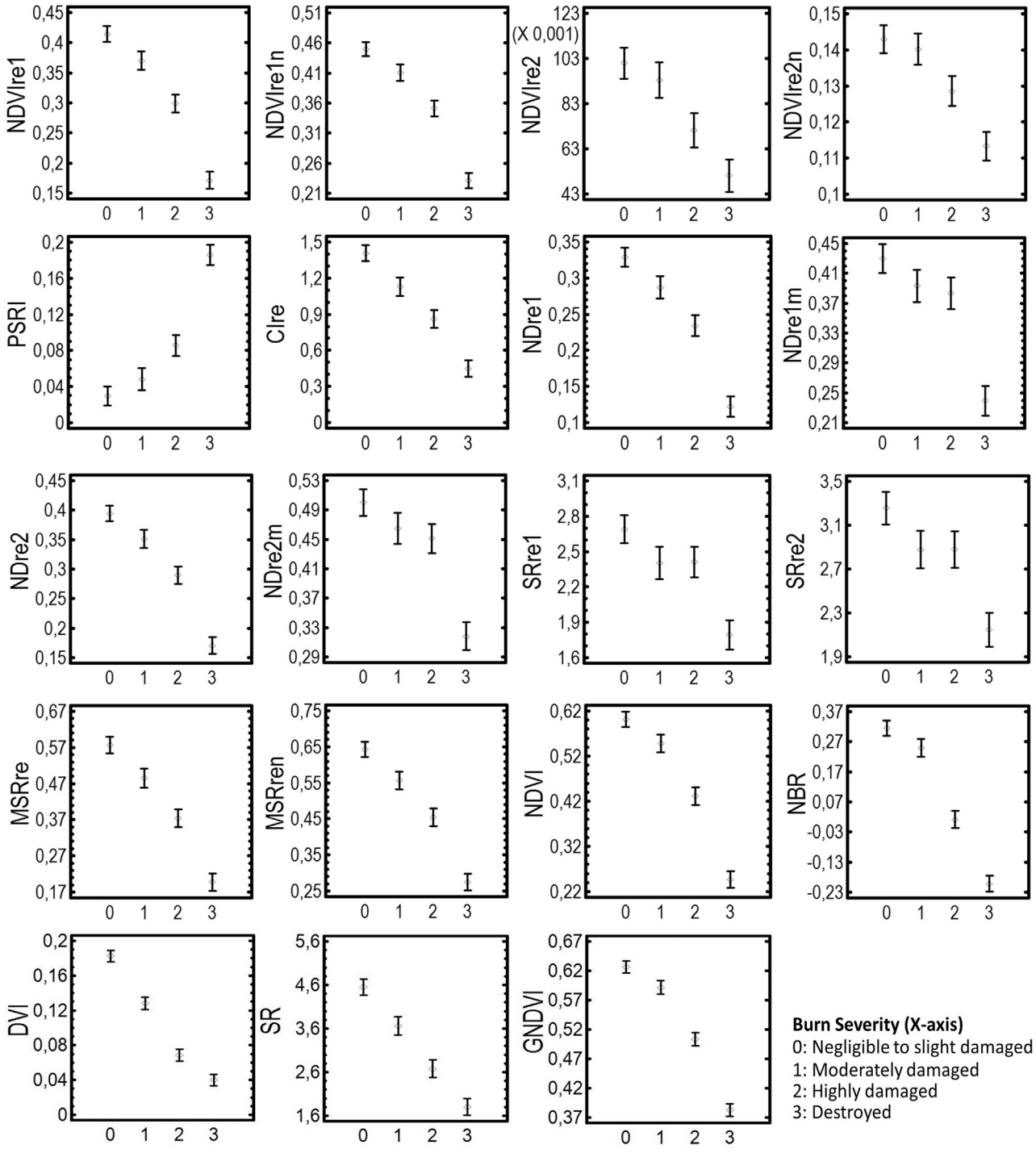

Fig. 3. Error-bar plots for the tested spectral indices (mean value and 95% Fischer's LSD interval of each burn severity set of reference plots).

Acknowledgement

The authors wish to thank two anonymous reviewers who significantly improved the quality of the manuscript.

References

Agresti, A., 2002. Categorical Data Analysis. Wiley-Interscience, Hoboken, New Jersey, pp. 710.

Barnes, E.M., Clarke, T.R., Richards, S.R., Colaizzi, P.D., Haberland, J., Kostrzewski, M., Waller, P., Choi, C., Riley, E., Thompson, T., Lascano, R.J., Li, H., Moran, M.S., 2000. Coincident detection of crop water stress, nitrogen status and canopy density using ground-based multispectral data. In: Proceedings 5th International Conference Precision Agriculture, Bloomington, USA, pp. 1–15.

Berger, M., Aschbacher, J. (Eds.), 2012. Remote Sens. Environ. 120, 1–276.

Birth, G., McVey, G., 1968. Measuring the color of growing turf with a reflectance spectrophotometer. Agron. J. 60, 640–643.

Buschmann, C., Nagel, E., 1993. In vivo spectroscopy and internal optics of leaves as basis for remote sensing of vegetation. Int. J. Remote Sens. 14, 711–722.

Chavez, P.S., 1996. Image-based atmospheric corrections—revisited and improved. Photogramm. Eng. Remote Sens. 62, 1025–1036.

Chen, J., 1996. Evaluation of vegetation indices and modified simple ratio for boreal applications. Can. J. Remote Sens. 22, 229–242.

Chuvieco, E., Riaño, D., Danson, F.M., Martín, P., 2006. Use of radiative transfer model to simulate to postfire spectral response to burn severity. J. Geophys. Res. 111, G04S09.

Chuvieco, E. (Ed.), 2009. Earth Observation of Wildland Fires in Mediterranean Ecosystems. Springer, New York.
Curran, P.J., Dungan, J.L., Gholz, G.H., 1990. Exploring the relationship between reflectance red edge and chlorophyll content in slash pine. Tree Physiol. 7, 33–48.
ESA, European Spatial Agency, 2015. Sentinel-2 user handbook. ESA Standard Document. 64.
Escuin, S., Navarro, R., Fernández, P., 2008. Fire severity assessment by using NBR (Normalized burn ratio) and NDVI (Normalized Difference Vegetation Index) derived from LANDSAT TM/ETM images. Int. J. Remote Sens. 29, 1053–1073.
Fletcher, K., 2012. Sentinel-2: ESA's Optical High-Resolution Mission for GMES Operational Services (European Spatial Agency SP-1322/2) ISBN 978-92-9221-419-7, ISSN 0379-6566.
Gitelson, A.A., Merzlyak, M., 1994. Spectral reflectance changes associated with autumn senescence of *Aesculus hippocastanum* L. and *Acer platanoides* L. leaves. Spectral features and relation to chlorophyll estimation. J. Plant Physiol. 143, 286–292.
Gitelson, A.A., Gritz, Y., Merzlyak, M., 2003. Relationships between leaf chlorophyll content and spectral reflectance and algorithms for non-destructive chlorophyll assessment in higher plant leaves. J. Plant Physiol. 160, 271–282.
Hill, M.J., 2013. Vegetation index suites as indicators of vegetation state in grassland and savanna: an analysis with simulated SENTINEL 2 data for a North American transect. Remote Sens. Environ. 137, 94–111.
Key, C.H., Benson, N.C., 2006. Landscape Assessment (LA). FIREMON: Fire effects monitoring and inventory system. Gen. Tech. Rep. RMRS-GTR-164-CD. U.S. Department of Agriculture, Forest Service, Rocky Mountain Research Station, Fort Collins, CO.
Korets, M.A., Ryzhkova, V.A., Danilova, I.V., Sukhinin, A.I., Bartalev, S.A., 2010. Forest disturbance assessment using satellite data for moderate and low resolution. In: Balzter, H. (Ed.), Environment Change in Siberia: Earth Observation, Field Studies and Modeling. Springer.
Merzlyak, J.R., Gitelson, A.A., Chivkunova, O.B., Rakitin, V.Y., 1999. Non-destructive optical detection of pigment changes during leaf senescence and fruit ripening. Physiol. Plant. 106, 135–141.
Segl, K., Guanter, L., Gascon, F., Kuester, T., Rogass, C., Mielke, C., 2015. S2eteS: an end-to-end modelling tool for the simulation of Sentinel-2 image products. IEEE Trans. Geosci. Remote Sens. 53, 5560–5571.
Shang, J., Liu, J., Ma, B., Zhao, T., Jiao, X., Geng, X., Huffman, T., Kovacs, J.M., Walters, D., 2015. Mapping spatial variability of crop growth conditions using RapidEye data in Northern Ontario, Canada. Remote Sens. Environ. 168, 113–125.
Sims, D., Gamon, J., 2002. Relationships between leaf pigment content and spectral reflectance across a wide range of species, leaf structures and developmental stages. Remote Sens. Environ. 81, 337–354.
Tucker, C.J., 1979. Red and photographic infrared linear combinations for monitoring vegetation. Remote Sens. Environ. 8, 127–150.
van der Meer, F.D., van der Werff, H.M.A., van Ruitenbeek, F.J.A., 2014. Potential of ESA's Sentinel-2 for geological applications. Remote Sens. Environ. 148, 124–133.
van der Werff, H.M.A., van der Meer, F.D., 2015. Sentinel-2 for mapping iron absorption feature parameters. Remote Sens. 7, 12635–12653.